

Sliding Mode Control of Three Levels Back-To-Back VSC-HVDC System Using Space Vector Modulation

Bouafia Saber*, **Benaissa Abselkader***, **Bouzidi Mansour*****, **Barkat Said*****

* Departement of Electrical Engineering, Intelligent Control & Electrical Power Systems Laboratory, University of Djilali Liabes, Sidi Bel Abbes, Algeria

** Department of Electrical Engineering, University of Kasdi Merbah Ouargla, Algeria

*** Departement of Electrical Engineering, M'sila University

Article Info

Article history:

Received Jan 3, 2014

Revised Feb 28, 2014

Accepted Mar 12, 2014

Keyword:

Sliding mode controller

Back-to-Back VSC-HVDC system

Capacitors voltages balancing

Multilevel space vector modulation

ABSTRACT

In this study, a sliding mode strategy proposed to control a three levels Back-to-Back High Voltage Direct Current (HVDC) system based on the three-level voltage source converter (VSC). The voltage-balancing control of two split DC capacitors of the VSC-HVDC system is achieved using three-level space vector modulation with balancing strategy based on the effective use of the redundant switching states of the inverter voltage vectors. Finally, a complete simulation of the VSC-HVDC system validates the efficiency of the proposed strategy law. Compared to the conventional control, Sliding Mode Control scheme for the VSC-HVDC system shows the attractive advantages such as offering high tracking accuracy, fast dynamic response and good robustness.

*Copyright © 2014 Institute of Advanced Engineering and Science.
All rights reserved.*

Corresponding Author:

Bouafia Saber,

Departement of Electrical Engineering,

Intelligent Control & Electrical Power Systems Laboratory,

University of Djilali Liabes, Sidi Bel Abbes

Sidi Bel Abbes 22000, BP 89 Algeria.

Email: bouafia.saber@gmail.com

1. INTRODUCTION

High Voltage direct Current (HVDC) power transmission systems and technologies constitute a key application of the power electronics technology to electrical power networks. The economics of bulk power transmission by underground means is increasingly moving in favor of direct current. The HVDC links have the ability to exert instantaneous power control in neighboring AC systems [1]-[2]. Great many research efforts have been directed towards realizing HVDC models for stability studies and power flows [2].

Fundamentally, two HVDC technologies are available [3]; (i) the conventional thyristor-based line commutated converter (LCC) HVDC which is a well-proven technology with the first application in 1954 in Gotland, Sweden. (ii) VSC-HVDC, which is a relatively new technology under rapid development. The VSC technology was initially developed for drive technologies due to significant increase in voltage and power ratings of semiconductors, such as the insulated gate bipolar transistor (IGBT), the VSC-HVDC scheme started to find applications in the late 1990s, especially where the interconnected AC networks had low short-circuit levels or where a small footprint was required [4]-[5].

The VSC offers several advantages over the LCC-HVDC scheme [3]-[4]; VSC uses self-commutated devices which give attractive features such as: the independent control of active and reactive power, the ability to supply passive loads and weak grids, and the ability to operate without external commutation voltage. Moreover, VSC has a relative small footprint due to the small size of the harmonic filters [3]-[4].

The requirement to meet high voltage levels, both at AC and DC sides, of an HVDC converter station is best accommodated by multilevel VSC configurations [4]. They were investigated with the requirement of quality and efficiency in high power systems. They offer many advantages such as increased power rating, minimized the harmonic effects and reduced electromagnetic interference (EMI) emission [4]. Recently, HVDC converter systems using full back-to-back multilevel NPC converters are being investigated owing to their high-voltage, high-current and staircase-like waveform capabilities [4]-[5]. Pulse width modulation (PWM) techniques are showing popularity to control multilevel inverters for multi-megawatt industrial applications [6]. Space vector modulation (SVM) is one of the most popular PWM techniques gained interest recently. The salient features of the SVM strategy are as follows. i) It minimizes total harmonic distortion of the ac-side voltages, through utilization of all available voltage levels of the VSC. ii) It minimizes the switching losses since, over each sampling period of the SVM modulator, it uses the three adjacent switching states with minimum ON-OFF state transitions of the switching devices. iii) It enables development of a method for dc-capacitor voltage balancing without the need for auxiliary power circuits and/or offline calculations [8].

The control system plays an important role in the whole HVDC system [6]-[8]. Good controllers can improve the operating characteristics not only of DC system itself, but also of AC systems. In control theory, sliding mode control, or SMC, is a nonlinear control method that alters the dynamics of a nonlinear system by application of a discontinuous control signal that forces the system to "slide" along a cross-section of the system's normal behavior [9]-[10].

In this study, sliding mode control strategy is applied to control a three-level back-to-back VSC-HVDC system in the aim to improve its performances. It will be used for developing the instantaneous active and reactive powers and DC voltage controllers.

2. SYSTEM STRUCTURE AND MATHEMATICAL MODEL OF VSC-HVDC BACK-TO-BACK SYSTEM

Figure 1 shows a schematic representation of a three-level VSC-based HVDC system. The system comprises two back-to-back connected three-level NPC converters units. The DC-link is composed of two nominally-identical capacitors.

The two VSC units share the same DC-capacitors and intermediate nodes O_1 are common between VSC-1 and VSC-2. An estimate of the total switching losses of the system is modelled by resistor R_p [4]. R_p is not shown in Figure 1. The AC-side terminal of each converter is connected to the corresponding AC system through a series connected R and L and a three-phase transformer. For simplicity and without the loss of generality, we assume the following: i) the voltage magnitudes of both grids are the same; however, the phases can assume any values. ii) The power switches, diodes and passive components of the two VSCs are correspondingly identical.

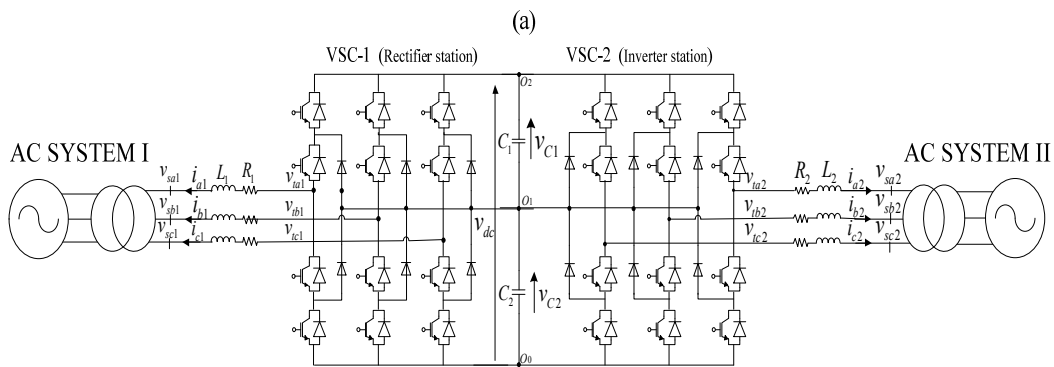


Figure 1. Three phase back-to-back three level NPC based VSC-HVDC system

To avoid repetitions in the formulation, the quantities of VSC-1 and AC system-1 are indexed by $k=1$, while those of VSC-2 and AC system-2 are indexed by $k=2$. In this paper, station 1 is designated and chosen as rectifier station while station 2 is designated as inverter station.

$$\begin{cases} \frac{di_{dk}}{dt} = -\frac{R_k}{L_k}i_{dk} + \omega i_{qk} + \frac{v_{tdk} - v_{sdk}}{L_k} \\ \frac{di_{qk}}{dt} = -\frac{R_k}{L_k}i_{qk} - \omega i_{dk} + \frac{v_{tqk} - v_{sqk}}{L_k} \\ \frac{dv_{dc}}{dt} = -\frac{1}{R_p C_{eq}} - \frac{2}{C_{eq}}i_{dc} \end{cases} \quad (1)$$

Where $C_{eq}=C/2$ is the DC-link equivalent capacitor. In the synchronous frame, v_{sdk} and v_{sqk} are the d , q axes components of the respective source voltages, i_{dk} and i_{qk} are that of the line currents, v_{tdk} and v_{tqk} are that of the converter input voltages. v_{dc} is the DC bus voltage and i_{dc} is equivalent DC current like in case of two level converter [8].

3. SLIDING MODE CONTROL OF BACK-TO-BACK VSC-HVDC SYSTEM

Figure 2 shows a schematic representation of a VSC-based HVDC system and its control structure diagram. The controls of a VSC-HVDC system is basically the control of the transfer of energy with independent control of active and reactive power and also keep the DC link voltage at the desired level to support the required active and reactive power commands [5]-[6].

From Equation (1), it is obvious that the converter is a nonlinear and coupled system. So a nonlinear controller based on the sliding mode method is developed in this section.

The system (1) is subdivided in three subsystems as follows:

Subsystem 1:

The first subsystem is characterized by only one state $x = v_{dc}$ and only one control input $u_1 = i_{dc}$.

$$\frac{dv_{dc}}{dt} = -\frac{1}{R_p C_{eq}} - \frac{2}{C_{eq}}i_{dc} \quad (2)$$

The Equation (2) can be written as follow:

$$\begin{cases} \dot{x}_1 = L_f h_1 + L_g h_1 u_1 \\ y_1 = h_1(x) = v_{dc}, \quad y_{1d} = v_{dc}^* \end{cases} \quad (3)$$

Where:

$$x_1 = v_{dc}, \quad u = i_{dc}, \quad L_f h_1 = -\frac{1}{R_p C_{eq}}, \quad L_g h_1 = -\frac{2}{C_{eq}}$$

Subsystem 2:

The second subsystem is also characterized by only one state $x = i_{dk}$ and only one control input $u = v_{tdk}$.

$$\frac{di_{dk}}{dt} = -\frac{R_k}{L_k}i_{dk} + \omega i_{qk} + \frac{v_{tdk} - v_{sdk}}{L_k} \quad (4)$$

The Equation (4) can also be written as follow:

$$\begin{cases} \dot{x}_2 = L_f h_2 + L_g h_2 u_2 \\ y_2 = h_2 = i_{dk}, \quad y_{2d} = i_{dk}^* \end{cases} \quad (5)$$

Where:

$$x_2 = i_{dk}, \quad u_2 = v_{tdk}, \\ L_f h_2(x) = -\frac{R_k}{L_k}i_{dk} + \omega i_{qk} - \frac{v_{sdk}}{L_k}, \quad L_g h_2 = \frac{1}{L_k}$$

Subsystem 3:

The third subsystem is also characterized by one state $x = i_{qk}$ and only one control input $u = v_{tqk}$.

$$\frac{di_{dk}}{dt} = -\frac{R_k}{L_k}i_{dk} + \omega i_{qk} + \frac{v_{tdk} - v_{sdk}}{L_k} \quad (6)$$

The Equation (6) can also be written as follow:

$$\begin{cases} \dot{x}_3 = L_f h_3 + L_g h_3 u_3 \\ y_3 = h_3 = i_{qk}, y_{3d} = i_{qk}^* \end{cases} \quad (7)$$

Where:

$$x_3 = i_{qk}, u_3 = v_{tqk},$$

$$L_f h_3(x) = -\frac{R_k}{L_k}i_{qk} + \omega i_{qk} - \frac{v_{sdk}}{L_k}, L_g h_3 = \frac{1}{L_k}$$

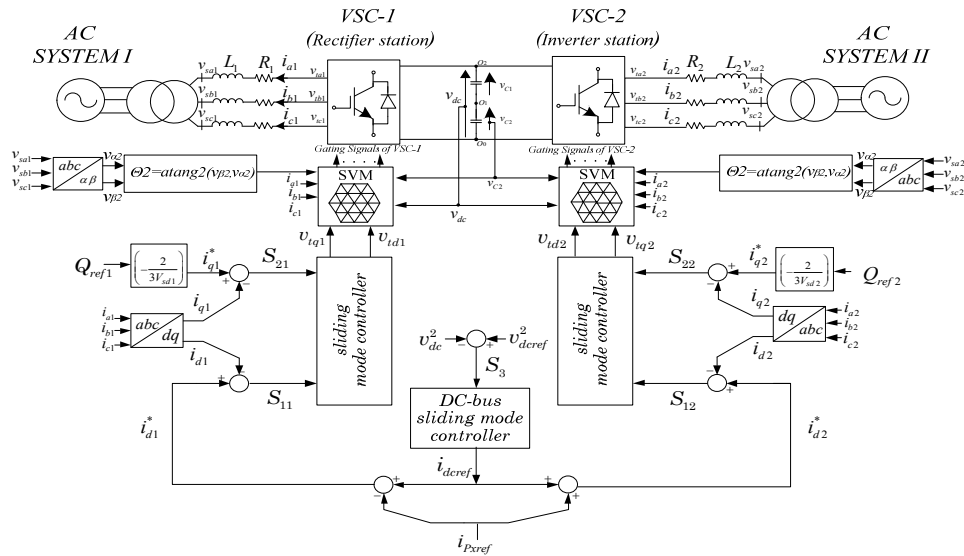


Figure 2. Control structure of the three levels VSC-HVDC system

For v_{dc} , i_{dk} and i_{qk} , the surfaces S_1 , S_2 and S_3 are given by the following expression:

$$\begin{aligned} S_1 &= k_1 (v_{dc} - v_{dc}^*) + k_{i1} \int (v_{dc} - v_{dc}^*) dt \\ S_2 &= k_2 (i_{dk} - i_{dk}^*) + k_{i2} \int (i_{dk} - i_{dk}^*) dt \\ S_3 &= k_3 (i_{qk} - i_{qk}^*) + k_{i3} \int (i_{qk} - i_{qk}^*) dt \end{aligned} \quad (8)$$

And consequently, their temporal derivatives are given by:

$$\begin{aligned} \dot{S}_1 &= k_1 \frac{d}{dt} (v_{dc} - v_{dc}^*) + k_{i1} (v_{dc} - v_{dc}^*) \\ \dot{S}_2 &= k_2 \frac{d}{dt} (i_{dk} - i_{dk}^*) + k_{i2} (i_{dk} - i_{dk}^*) \\ \dot{S}_3 &= k_3 \frac{d}{dt} (i_{qk} - i_{qk}^*) + k_{i3} (i_{qk} - i_{qk}^*) \end{aligned} \quad (9)$$

The equivalent control can be calculated from the formula $\dot{S} = 0$, and the stabilizing control is given to guarantee the convergence condition [6]-[11]. Finally, the control law is given by:

$$\begin{aligned} i_{vc}^* &= \frac{1}{L_g h_1} \left(\left(-L_f h_1 + \frac{dv_{dc}^*}{dt} \right) - \frac{k_{i1}}{k_1} (v_{dc} - v_{dc}^*) \right) - k_{dc} \text{sign}(S_1) \\ v_{idk}^* &= \frac{1}{L_g h_2} \left(\left(-L_f h_2 + \frac{di_{dk}^*}{dt} \right) - \frac{k_{i2}}{k_2} (i_{dk} - i_{dk}^*) \right) - k_{dk} \text{sign}(S_2) \\ v_{iqk}^* &= \frac{1}{L_g h_3} \left(\left(-L_f h_3 + \frac{di_{qk}^*}{dt} \right) - \frac{k_{i3}}{k_3} (i_{qk} - i_{qk}^*) \right) - k_{qk} \text{sign}(S_3) \end{aligned} \quad (10)$$

Where: $k_{dc}, k_{dk}, k_{qk}, k_{i1}, k_{i2}, k_{i3}, k_1, k_2$ and k_3 are positive constants.

4. THREE-LEVEL SPACE VECTOR MODULATION

A three-level converter differs from a conventional two-level converter in that it is capable of producing three different levels of output phase voltage. With three possible output states for each of the three phases, there are a total of 27 (3³) possible switch combinations. The result of plotting each of the output voltages in a $\alpha\beta$ reference frame is shown in Figure 3.

Figure 4 shows that the 27 switch combinations result in a total of 19 unique voltage vectors since some of the combinations produce the same voltage vector.

These different combinations relate to different ways of connecting the VSCs to the DC bus that result in the same voltage being applied to AC systems. Projection of the vectors on a $\alpha\beta$ coordinates forms a two-layer hexagon centered at the origin of the $\alpha\beta$ plane. Zero voltage vectors are located at the origin of the plane. The switching states are illustrated by 0, 1 and 2 which denote corresponding switching states. Any sampling instant the tip of the voltage vector is located in a triangle formed by three switching vectors nearest to the voltage vector (Figure 3). The nearest three vectors are chosen by determining the triangle within the vector space in which the desired voltage vector resides.

The required on duration of each of the vectors is determined by Equation (24). These specify that the demand vector, v_{ref} , is the geometric sum of the chosen three vectors (v_1, v_2, v_3) multiplied by their on-durations (d_1, d_2, d_3) and that their on-durations must fill the complete cycle.

$$\begin{cases} v_1 d_1 + v_2 d_2 + v_3 d_3 = v_{ref} T \\ d_1 + d_2 + d_3 = T \\ v_{ref} = |v_{ref}| e^{j\theta}, \theta = \angle v_{ref} \end{cases} \quad (11)$$

The next step is to identify the appropriate redundant switching states and generate the switching pattern to control voltages of the capacitors. This requires knowledge of phase currents and impacts of different switching states on dc-side intermediate branch currents and consequently capacitor voltages [6]-[7].

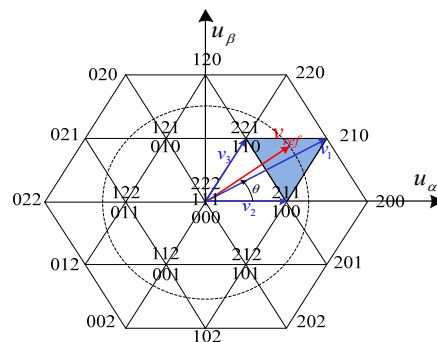


Figure 3. Space vector diagrams of three-level converter

5. DC-CAPACITOR VOLTAGES BALANCING STRATEGY

In a three-phase three-level VSC converter, the total energy E of DC-link capacitors is [7]:

$$E = \frac{C}{2}(v_{C1}^2 + v_{C2}^2) \quad (12)$$

When all capacitor voltages are balanced, the total energy E reaches its minimum of $E_{\min} = Cv_{dc}^2/4$, [7]-[8]. This condition is called the minimum energy property which can be used as the basic principle for DC-capacitor voltage balancing and control. The adopted control method should minimize the quadratic cost function J associated with voltage deviation of the DC-capacitors [8]. The cost function is defined as follows:

$$J = \frac{C}{2}(\Delta v_{C1}^2 + \Delta v_{C2}^2) \quad (13)$$

Where: $\Delta v_{Cj} = v_{Cj} - \frac{v_{dc}}{2}$, $j=1,2$

Based on proper selection of redundant switching states of both VSC units, J can be minimized, if capacitor voltages are maintained at voltage reference values of $v_{dc}/2$. The mathematical condition to minimize J is:

$$\Delta v_{C2} (\bar{i}_{x1}(k) + \bar{i}_{x2}(k)) \geq 0 \quad (14)$$

Where Δv_{C2} is the voltage drift at sampling period k . Currents components $x=1,2,3$ are computed for different combinations of adjacent redundant switching states over a sampling period and the best combination which maximize (14) is selected.

6. RESULTS AND ANALYSIS

To validate the developed steady state model and a control strategy, its performance and robustness are analyzed when applied SMC of Three Levels Back-To-Back VSC-HVDC System Using Space Vector Modulation with the parameters presented in Table 1 [7]. Simulation studies of the system are executed using MATLAB™/SIMULINK for different operating conditions, the system was simulated during 0.1s.

The HVDC system of Figure 1 is capable to interface the two AC systems with different nominal frequencies and maintain DC-voltage balance [6]. To demonstrate this capability, dynamic response of the system of Figure 1 to steps changes in real and reactive power demands is considered. The nominal frequencies of AC system-1 and AC system-2 of Figure 1 are 60Hz and 50Hz respectively.

Table 1. Simulation Parameters

Parameters of the Study System	Value
Each DCC nominal power	110 MW
Each AC system nominal voltage	138 kV
Each AC system Short Circuit Ratio	5
Nominal Frequencies f_1	60 Hz
Nominal Frequencies f_2	50 Hz
Each transformer voltage ratio	138 kV / 30 kV
R_1 and R_2	40 mΩ
L_1 and L_2	6 mH
Nominal net DC voltage	30 kV
Resistance R_p	1.8 K Ω
VSC-1 sampling frequency	2520 Hz
VSC-2 sampling frequency	2520 Hz
DC-link Capacitor C_1, C_2	2000 μF

6.1. Real Power Control

Initially, the system is in a standby mode of operation and v_{dcref} is set to 30kV. Both VSCs units operate at unity power factor. At $t = 0.04$ s up to 0.07 s, P_{ref2} is changed as a step corresponding to a power change from 0 to 10 Mw, from AC system-1 to AC System-2. At $t = 0.07$ s, P_{ref2} is changed from 10Mw

to -10Mw; this change corresponds to a power flow reversal from 10Mw to -10Mw, from AC system-2 to AC system-1.

6.1. Reactive Power Control

in the first time interval, between 0 and 0.05 s, the system is in stop mode; at t = 0.05 s, reactive power demands of AC systems 1 are changed from 0 to -5 Mvar and from 0 to 3 Mvar for ac system-2.

The performance of the proposed SMC control will be carried out through simulation study as well as to be compared with that of linear control. The results under the conventional PI control will be given. Then comparisons are made between these two controls:

- Control 1: Sliding mode Control in rotating synchronous frame.
- Control 2: Conventional PI control in rotating synchronous frame.

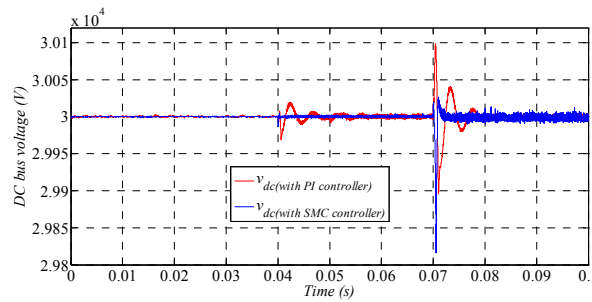


Figure 4. Simulation results of DC-Link voltage

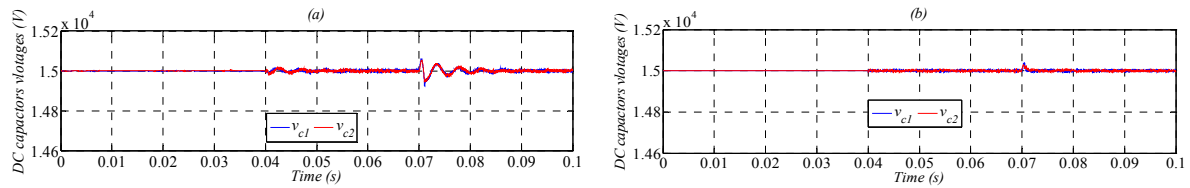


Figure 6. Simulation results of DC capacitors voltages (a) using PI controller, (b) using SMC controller

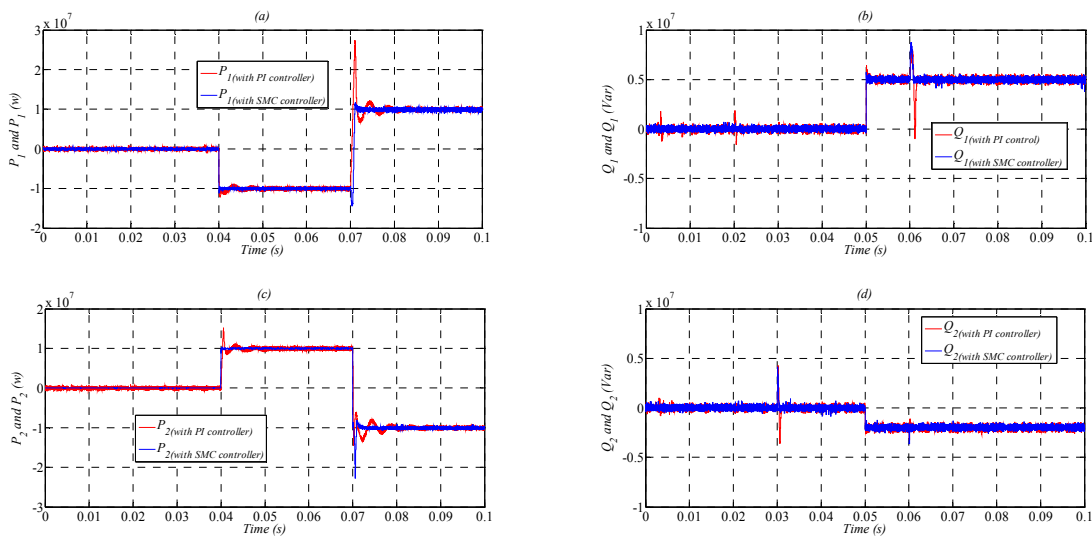


Figure 7. System responses using PI controller and SMC controller (a) of Real power for at AC system 1 side, (b) of Reactive power for at AC system 1 side, (c) of Real power for at AC system 2 side 1, (d) of Real power for at AC system 2 side

Figure 4 and 5 shows the DC voltage response with PI and nonlinear controllers, we can observe that the DC-bus voltage is maintained close to its reference with good approximation, stability and without overshoot in case of SMC controller, it is important also to note that the application of the proposed redundant vectors based three-level SVM control maintains capacitors voltages balanced to their references of $v_{dc}/2$. It is possible to see how the voltage across each capacitor remains constant after the perturbation is applied. This result confirms the effectiveness of Sliding mode DC voltage controller.

Figure 7 shows dynamic response of the system under various steps changes in real and reactive power demands of the HVDC system for SMC and PI controllers respectively. We can show that real and reactive power and current components of AC system 1 and AC system 2 are regulated at the corresponding references, and are well decoupled from each other.

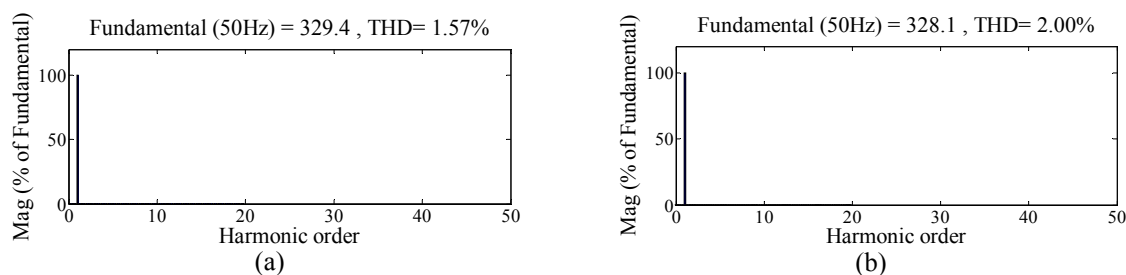


Figure 8. Harmonic spectrum of line current (a) with PI Controller, (b) with SMC controller

Figure 8(a) and 8(b) shows harmonic spectrum of line current demonstrate that the distortion in supply current with SMC strategy where total harmonic distortion (THD) equal to 1.57% is less than in case of PI controller where THD=2.00% .

7. CONCLUSION

In this paper, Sliding Mode control strategy applied to a back-to-back three level voltage source converter HVDC system using space vector modulation. The effectiveness of the proposed control strategy under various operating conditions is analyzed and compared with conventional controller based on simulation studies in the MATLAB™/SIMULINK environment.

Simulation results indicate that the performances of SMC strategy are much better than the above linear control with conventional controller during active and reactive power change. The absence of overshoots in DC voltages responses during powers changes, good transient responses and low current distortion demonstrates the superiority of the SMC strategy compared to its counterpart traditional PI controller. So SMC scheme for the VSC-HVDC system shows some attractive advantages such as offering high tracking accuracy, fast dynamic response and good robustness.

REFERENCES

- [1] K Meah, S Ula. Comparative Evaluation of HVDC and HVAC Transmission Systems. *IEEE Power Engineering Society General Meeting*, Tampa, FL, USA. 2007: 1-5.
- [2] J Arrillaga, YH Liu, NR Watson. Flexible Power Transmission The HVDC Options. *John Wiley and Sons, LTD.* 2007.
- [3] Nagu B, Ramana Rao PV, Sydulu M. Enhancement of AC System Stability using Artificial Neural Network Based HVDC Controls. *International Journal of Electrical and Computer Engineering (IJECE)*. 2013; 3(4): 441 - 455.
- [4] M Barnes, A Beddard. Voltage Source Converter HVDC Links – The state of the Art and Issues Going Forward. *Energy Procedia*. by Elsevier Ltd. 2012; 24: 108- 122.
- [5] I Colak, E Kabalci, R Bayindir. Review of multilevel voltage source inverter topologies and control schemes. *Energy Conversion and Management*. Elsevier Ltd. 2011; 52: 1114–1128.
- [6] B Parkhideh, S Bhattacharya. *A Practical Approach to Controlling the Back-to-Back Voltage Source Converter System*. Industrial Electronics, 34th Annual Conference of IEEE. Orlando, FL, USA. 2008: 514 - 519.
- [7] A Tyagi, KR Padiyar. Dynamic analysis and simulation of a VSC based Back-to-Back HVDC link. *Power Electronics, IICPE*. Chennai, India. 2006: 232- 238.

- [8] M Saeedifard, R Iravani R, Pou J. A space vector modulation strategy for a back-to-back five-level HVDC converter system. *IEEE Trans. Ind. Electron.*, 2009; 56: 452–466.
- [9] HA Hotait, AM Massoud, SJ Finney, BW Williams. Capacitor Voltage Balancing Using Redundant States of Space Vector Modulation for Five-Level Diode Clamped Inverters. *IET Power Electronics*. 2010; 3(2): 292–313.
- [10] Bouzidi Mansour, Benaissa Abselkader, Barkat Said. Sliding mode Control using 3D-SVM for Three-phase Four-Leg Shunt Active Filter. *International Journal of Power Electronics and Drive System (IJPEDS)*. 2013; 3(2): 147–154.
- [11] S Elangovan, K Baskaran. Sliding mode controller and simplified space vector modulator for three phase shunt active power filter. *IEEE International Conference on Power Electronics, IICPE*. India. 2006; 315-318.
- [12] N Sabanovic Behlilovic, T Ninomiya, A Sabanovic, B Perunicic. Control of Three-Phase Switching Converters: A Sliding Mode Approach. *IEEE Power Electronics Specialists Conference (PESC)*. 1993; 630-635.